

Dual nature of the ferroelectric and metallic state in LiOsO₃Gianluca Giovannetti^{1,2} and Massimo Capone¹¹*CNR-IOM-Democritos National Simulation Centre and International School for Advanced Studies (SISSA),
Via Bonomea 265, I-34136 Trieste, Italy*²*Institute for Theoretical Solid State Physics, IFW-Dresden, PF 270116, 01171 Dresden, Germany*

(Received 30 April 2014; revised manuscript received 21 October 2014; published 10 November 2014)

Using density functional theory we investigate the lattice instability and electronic structure of recently discovered ferroelectric metal LiOsO₃. We show that the ferroelectric-like lattice instability is related to the Li-O distortion modes while the Os-O displacements change the *d-p* hybridization as in common ferroelectric insulators. Within the manifold of the *d* orbitals, a dual behavior emerges. In the ferroelectric transition the empty *e_g* orbitals change their hybridization with the oxygen *p* orbitals, while the *t_{2g}* orbitals are responsible for the metallic response. Interestingly, these orbitals are nominally half filled by three electrons, a configuration which suffers from strong correlation effects even for moderate values of the screened Coulomb interaction.

DOI: [10.1103/PhysRevB.90.195113](https://doi.org/10.1103/PhysRevB.90.195113)

PACS number(s): 77.80.B–, 71.45.Gm, 77.84.–s

I. INTRODUCTION

Ferroelectric and multiferroic materials represent a fascinating ground where an immense applicative potential [1] emerges from the competition between different interactions with an intimate interplay of spin, charge, orbital, and lattice degrees of freedom. In a prototype example of ferroelectric system, the *d*⁰ perovskite BaTiO₃, the ferroelectric distortion is driven by the hybridization between the filled oxygen *2p* states and the nearly empty *d* states of the transition metal (TM) cation. The ferroelectric displacement reduces the distance between the TM cation and one or more of the surrounding oxygen anions leading to gain in covalent bond energy. This effect leads to a maximum energy gain for empty *d* orbitals, because the oxygen electrons populate only the bonding combination, but it is expected to survive for sufficiently low filling of the TM orbitals, when only a small fraction of the antibonding combinations is populated. The fact that this mechanism for ferroelectricity requires a nearly unoccupied *d* shell of the TM cations while a partial filling of these electronic *d* states is required to have a magnetic moment explains the incompatibility between ferroelectricity and magnetism and the reason of scarcity of multiferroic materials.

From this perspective, CaMnO₃ is an interesting counterexample. Here Mn is a *d*³ configuration yet it simultaneously displays ferroelectricity and magnetic ordering. This is understood by observing that the empty *e_g* orbitals hybridize with the oxygen *p* orbitals leading to ferroelectric distortions, while the half-filled *t_{2g}* orbitals give rise to the magnetic ordering [2,3]. Therefore, while BaTiO₃ is a band insulator due to the *d*⁰ configuration, the insulating state of CaMnO₃ is dominated by the strong correlation in the *t_{2g}* manifold [4].

On the other hand, metals are not expected to exhibit ferroelectricity because the itinerant electrons screen the electric fields and inhibit the electrostatic forces responsible for ferroelectric distortions. The concept of a “ferroelectric metal” was however theoretically proposed in 1965 by Anderson and Blount [5], who have shown that the loss of a center of symmetry in a metal is possible only through a second-order phase transition. The pyrochlore compound Cd₂Re₂O₇ appeared as possible realization because it displays an unusual structural transition in its metallic state, but a unique polar

axis could not be identified [6,7]. For electron-doped BaTiO₃ ferroelectric distortions occur in two distinct metallic and insulating phases that do not coexist microscopically [8,9].

A first success has been recently obtained in the search for a ferroelectric metal. LiOsO₃ displays indeed metallic conduction while a second-order phase transition to a state where the ionic structure breaks the lattice symmetry occurs at *T_s* = 140 K [10]. Neutron and x-ray diffraction studies show indeed that at *T_s* the space group changes from centrosymmetric *R* $\bar{3}c$ to ferroelectric-like *R3c* [10].

In this paper we investigate the electronic structure of metallic LiOsO₃ and we address the driving force behind the ferroelectric instability by means of density functional theory calculations. We find that the ferroelectric-like distortions are mainly related to the Li-O modes while Os-O displacements enhance the hybridization between the *e_g* orbitals of Os and the *p* orbitals of O. The three electrons populating the *t_{2g}* orbitals are instead responsible for the metallic behavior. As opposed to the case of CaMnO₃, the strength of the electron-electron interactions is not sufficient to drive a metal-insulator transition, and the system remains a correlated metal. Interestingly, such correlated state is not unstable to a Stoner-like antiferromagnetic state because the band structure strongly breaks particle-hole symmetry and remains metallic. The stabilization of the ferroelectric structure in LiOsO₃ coexisting with metallic conductance is the consequence of a near decoupling between the metallic electrons in the *t_{2g}* electrons from the soft phonons which break the inversion symmetry [11].

The paper is organized as follows. Section II introduces the structure of the system and our strategy to study ferroelectricity within DFT. Section III presents our characterization of the ferroelectric instability. Section IV is devoted to the investigation of the role of electron correlations in the metallic state, while Sec. V contains the final conclusions.

II. STRUCTURE AND METHODS

In Fig. 1(a) we display the crystal structure of LiOsO₃, which is a standard perovskite composed by oxygen octahedra sharing the corner atoms. In the *R* $\bar{3}c$ centrosymmetric structure the Os atoms are at the center of the octahedra and all the

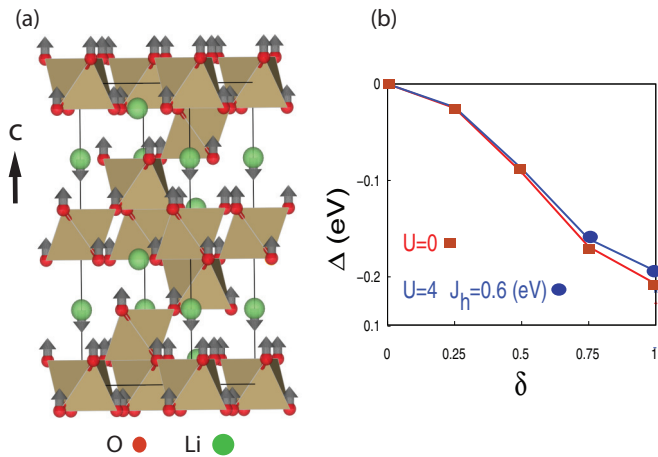


FIG. 1. (Color online) (a) Ionic displacements (arrows) along the polar axis c in the noncentrosymmetric structure of LiOsO_3 . (b) Total energy gain (Δ) due to the ferroelectric-like distortions calculated within LDA as a function of the distortion δ ($\delta = 1$ corresponds to the experimental distorted structure).

distances with surrounding O atoms are equal, while Li atoms are located halfway between two neighboring octahedra in the direction of the c axis.

The loss of symmetry in the $R3c$ space group involves the ferroelectric displacements of Li and O atoms along the polar axis c . As a consequence the Os atoms become off-centered, while the Li atoms are ferroelectrically displaced with respect to the oxygen planes [see the arrows in Fig. 1(a)]. This structural transition is very similar to that observed in the isostructural compound LiNbO_3 , where the ferroelectric state can be understood in terms of Nb-O hybridization [12].

We start our investigation performing density functional theory calculations (DFT) [13] for the refined experimental structures with space groups $R\bar{3}c$ and $R3c$ using the Vienna *Ab initio* Simulation Package [14]. Our DFT simulations are performed within the local density approximation (LDA) [15] to the exchange-correlation potential. In a second step we supplement the LDA calculations by including also a Hubbard-like interaction and the Hund's exchange term J_H on Os d orbitals within the LDA+ U scheme [16]. The cutoff for the plane-wave basis set is 500 eV and a $12 \times 12 \times 8$ mesh is used for the Brillouin-zone sampling. We perform atomic relaxations until the change in total energy is less than 10^{-6} eV. The check of the symmetry is performed with the program FINDSYM [17].

III. THE FERROELECTRIC INSTABILITY

To study the structural ferroelectric instability we consider the refined experimental structure with the space group $R3c$. A relaxation of the ionic coordinates gives rise to essentially negligible variations and confirms the stability of the experimental $R3c$ structure within DFT [18]. The overall results agree with previous *ab initio* calculations showing that the soft A_{2u} mode at the zone center is responsible for the noncentrosymmetric transition [19,20].

In order to identify the nature of the ferroelectric-like distortions and the contribution of the different ions, we

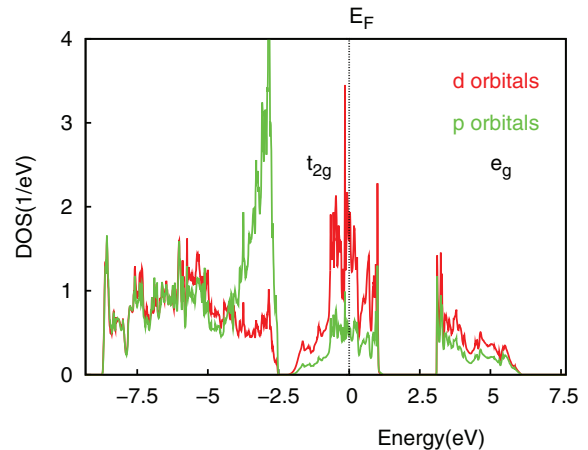


FIG. 2. (Color online) Orbital-resolved density of states for d and p orbitals within LDA. The Fermi level is the zero of the energy axis.

construct a putative structure with $R\bar{3}c$ symmetry [21] starting from the relaxed $R3c$ structure by means of the PSEUDO program [22]. Such a symmetrized structure allows for a direct comparison of energies with the distorted one and it is extremely close to the experimental centrosymmetric structure. Comparing the $R3c$ and $R\bar{3}c$ structures, we identify that the ferroelectric-like distortions are of mirror symmetry along the a and b unit cell vectors while along the polar axis c the displacements of Li, Os, and O ions are respectively 0.449, 0.002, and -0.028 Å. The breaking of the crystal symmetry is due to the different magnitude and direction of the Li and O displacements.

We define δ as a parameter measuring the distortions such that $\delta = 0$ corresponds to the centrosymmetric ionic positions while $\delta = 1$ corresponds to the ferroelectric ionic positions. The variation of the total energy $\Delta = E(\delta) - E(0)$ [$E(\delta)$ being the total energy for a given distortion] along the path connecting the centrosymmetric ($\delta = 0$) and ferroelectric ($\delta = 1$) ionic structures show that the fully distorted structure is clearly energetically favored and it gains 0.2 eV per unit cell within LDA, as shown in Fig. 1(b) (note that there are 6 Os ions in the unit cell).

The density of state we obtain in LDA, shown in Fig. 2, is clearly that of a metal, in agreement with experiments and previous electronic-structure calculations [10,19,20]. If we resolve the density of states separating the contribution of Os d orbitals and O p orbitals, we clearly see that in the whole relevant energy window the two degrees of freedom are strongly mixed. This clearly demonstrates a large d - p hybridization. Interestingly, the hybridization does not change much across the ferroelectric transition, similarly to what happens in other ferroelectrics BaTiO_3 , PbTiO_3 , and LiNbO_3 [12,23].

In order to better understand the electronic phenomena underlying the ferroelectric transition, we derive a tight-binding model by building maximally localized Wannier orbitals [24] choosing an energy window which includes bands originating from all the d orbitals of Os around the Fermi level (t_{2g} and e_g manifolds in Fig. 2). A first observation is that the crystal-field splitting between the t_{2g} and e_g orbitals is rather large (~ 4 eV) and gives rise to a clear separation between

the spectral feature around the Fermi level, which has mainly t_{2g} character and a higher-energy structure of e_g character. Os has a nominal valence of $5+$, so that 3 electrons have to fill the t_{2g} and e_g orbitals. A count of the bands lying in the energy window labeled as t_{2g} around the Fermi level (see Fig. 2) clearly shows that this manifold is actually able to host up to six electrons and it is therefore half filled by the three electrons, which leaves the high-energy e_g band empty. It is important to notice that we are not in principle allowed to label the levels as t_{2g} and e_g , as the symmetry breaking associated with the ferroelectric distortion mixes the two manifolds. Yet, the separation between a threefold manifold and a twofold one is evident in the band structure, suggesting that the above distinction still holds almost perfectly.

The d^3 configuration of LiOsO_3 with “ t_{2g} ” close to half filled and “ e_g ” close to be empty, as for CaMnO_3 [2,3], can be described as an e_g^0 electron configuration, with an empty set of bands well separated from the others, analogously to the d^0 configuration of most perovskite ferroelectric insulators. Then the empty e_g states can in principle provide the increase in bond energy required for the ferroelectric instability by hybridizing with the p orbital.

In order to identify how the above described electronic structure leads to the ferroelectric instability, in Fig. 3(a) we show the total energy variations Δ as a function of the ferroelectric distortions separated in contributions coming from Li-O, Li, and Os-O modes. Li-O mode refers to the case where the Os displacement is neglected, Li mode refers to the case where only Li displacements are considered, while in the case of Os-O mode the Li displacements are neglected. The energy gain is dominated by the displacement of the Li and O ions with a smaller energetic contribution from O displacements and a main contribution associated with the displacement of ions. Indeed the pure Li-O mode accounts for almost the full energy gain due to the ferroelectric distortion of LiOsO_3 . The Li and O displacements are then responsible for the ferroelectric transition in LiOsO_3 as already pointed from previous density functional theory calculations [19,20].

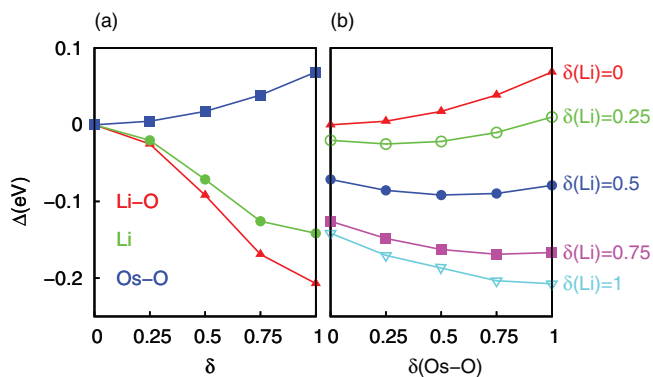


FIG. 3. (Color online) (a) Total energy gain Δ as a function of the displacements of selected atoms in the soft A_{2u} mode. We compare the results obtained for Li-O, Os-O, and Li modes, showing that most of the energetic gain comes from the Li-O mode. (b) Total energy gain as a function of the displacement of the Os-O mode [$\delta(\text{Os-O})$] for different fixed value of the Li-O displacement [$\delta(\text{Li-O})$]. The Os-O displacement leads to an energy gain only if also the Li atom is displaced.

The Os-O mode instead would lead to an energy increase in the absence of Li displacement. However the situation changes, as shown in panel (b) of Fig. 3, when the Li atom is displaced. Indeed, plotting Δ as a function of the ferroelectric distortions of the pure Os-O modes [$\delta(\text{Os-O})$] for different fixed values of the Li displacement, we find that the Os-O mode leads to an energy gain when the Li atoms are also displaced, with a maximum gain for the fully displaced case [$\delta(\text{Li}) = 1$].

This motion of Os and O atoms can indeed be directly linked to the hybridization between these atoms. Indeed Li atoms do not play a major role in the electronic structure around the Fermi level because of their nominal charge of $+e$ (corresponding to an empty s level). Indeed the bands with main Li character lie far below the Fermi level while the states at the Fermi level originate mainly from the hybridization of Os and O atoms. Our results then demonstrate that there is a cooperative and coupled displacement of Li and O ions, such that the shift of Li atoms gives the possibility to gain in the energy from the d - p hybridization of Os and O atoms. Such energy gain along the ferroelectric transition is however smaller if compared with the energy gain due to the Li displacements and it is consistent with the small changes of the hybridization between d (Os) and p (O) orbitals in the DOS. The latter mechanism based on d - p hybridization is common with many different ferroelectric insulators and in particular in LiNbO_3 [12,23].

IV. CORRELATION EFFECTS IN THE METALLIC STATE

Despite its metallic nature, LiOsO_3 has a residual resistivity more than one order of magnitude larger than that expected for a normal metal [10] and the spin susceptibility shows a Curie-Weiss behavior signaling the existence of local magnetic moments, even if an ordered magnetic moment larger than $0.2 \mu_B$ is experimentally excluded [10]. This observation suggests a bad metallic behavior which can be ascribed to the effects of electron-electron correlations pushing the system close to a Mott transition.

Indeed, although the $5d$ orbitals are usually spatially extended and in LiOsO_3 the delocalization is even more enhanced from hybridization with oxygen orbitals, electron correlations can still play an important role [25] in $5d$ systems, and in particular in LiOsO_3 because the t_{2g} orbitals are close to half filling, the electronic configuration which maximizes the correlation effects. The accurate value of the Hubbard U is not known for perovskite osmates, but it is not expected to exceed the range of values estimated for the iridates Sr_2IrO_4 and Ba_2IrO_4 [26], respectively 1.4 and 2.4 eV. This value has to be compared with an LDA bandwidth of around 3 eV for the t_{2g} bands. We now investigate whether this intermediate level of correlation affects the electronic properties of LiOsO_3 .

As a first step, we perform local spin-density approximation (LSDA) calculations with ferromagnetic (all spins are parallel) and G-type antiferromagnetic (every spin is antiparallel to all its neighbors) magnetic structures without finding any stable solution, ruling out a pure Slater antiferromagnetism arising from nesting of the Fermi surface. We then perform calculations by including the local Coulomb interactions between the Os d electrons, namely the Hubbard U and the Hund’s coupling starting from the experimental structure.

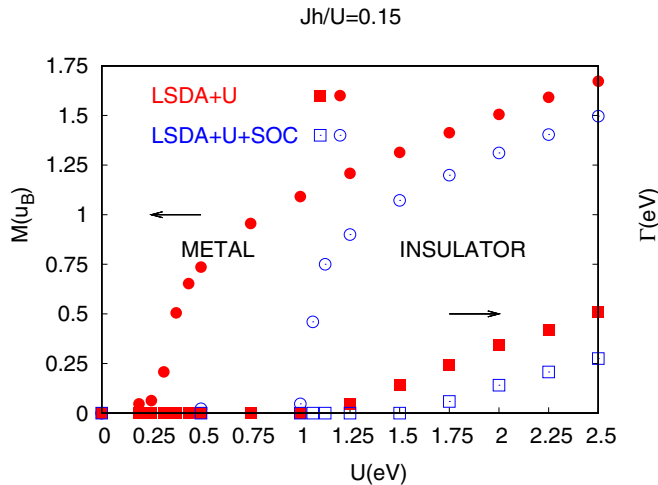


FIG. 4. (Color online) Magnetization M and charge gap Γ as a function of U within LDA+ U and LDA+ U +SOC calculations at fixed ratio $J_H/U = 0.15$.

U ranges from 0 to 2 eV and the ratio J_H/U is fixed at 0.15. We have checked that our conclusions are not strongly dependent on the value of J_H .

The energy gain due to the ferroelectric distortion is slightly reduced by electronic interactions [see Fig. 1(b)]. Within LDA+ U calculations a *metallic* G-type magnetic structure with local magnetic moments M smaller than $1 u_B$ can be stabilized at U values smaller than 1 eV (see Fig. 4). At a moderate value of U close to 1 eV, the G-type solution becomes insulating with a small but finite charge gap Γ (see Fig. 4). As shown in Fig. 4 M and Γ both increase upon increasing the electron-electron interactions U and J_H .

Our LDA+ U calculations finding a stable G-type magnetic structure and a metal-insulator transition at increasing value of U are not meant to prove a magnetic ordering, but they are rather instrumental to establish a significant role of electron-electron correlation in the t_g manifold. The Hartree-Fock treatment of correlations in LDA+ U naturally overestimates ordered phases, which have not been observed experimentally (even if an ordered magnetic moment smaller than $0.2 u_B$ is compatible with the experimental statistics [10]). On the other hand, these calculations show that the half-filled t_{2g} manifold is sensitive to correlation effects, which appear as the underlying physics behind the bad metallic behavior with local magnetic moments.

Our calculations therefore highlight a significant role of electron-electron correlations, even if the strength is not sufficient to drive a Mott transition in the correlated manifold. From this point of view, the theoretical description of LiOsO₃ and of its metallic phase requires a more accurate treatment of correlations such as dynamical mean-field theory. In this delicate metallic regime, it would also be important to accurately estimate the values of the interaction terms U and J_H .

V. EFFECT OF THE SPIN-ORBIT COUPLING

As the spin-orbit coupling (SOC) in the $5d$ transition-metal elements is expected to be strong, to study the interplay of electron correlations and spin-orbit interactions we performed LDA+SOC and LDA+ U +SOC calculations. Comparing the results for the nonmagnetic state with and without SOC, we find SOC to have a small effect of the shape of the band dispersion but the bandwidth of t_{2g} orbitals to be increased by 0.25 eV (not shown). The ratio between bandwidth of t_{2g} orbitals and the Coulomb interactions, namely U , controls the metal-insulator transition and as a consequence we find indeed that the critical U to drive the metallic state into a Mott transition is now pushed towards higher values (see Fig. 4). The obtained orbital moment for LiOsO₃, as for NaOsO₃ [27,28], is much smaller than its spin moment, showing that SOC effect for this $5d^3$ electronic configuration case is less strong with respect to the $5d^5$ case of Sr₂IrO₄ [29].

VI. CONCLUSIONS

In conclusion, we investigate the ferroelectric transition and electronic structure of LiOsO₃. We find the Li-O distortion modes to be responsible for ferroelectric-like instability while the Os-O distortions favor the hybridization of Os d states and O p states as in common ferroelectric insulators. Here the nearly empty e_g orbitals hybridize with the oxygen p orbitals contributing to the ferroelectric distortions, while the nearly half-filled t_{2g} orbitals are associated with the metallic response. Our study implies that the lattice and electronic degrees of freedom involved respectively in the ferroelectric transition and metallic ground state are weakly coupled in the second-order ferroelectric-like phase transition. The metallic state is associated with a nearly half-filled manifold of “ t_{2g} ” bands, in which the effect of electron correlations are expected to be particularly strong. Indeed even the moderate electron-electron interactions that we expect for this compound lead to a highly correlated metal which is expected to display a high resistivity and incipient magnetic moments even in the absence of an ordered magnetic moment. Interestingly, the system remains metallic despite the half-filling configuration because of the strong asymmetry of the density of states associated with the hybridization. Finally the spin-orbit coupling interaction increasing the bandwidth of t_{2g} manifold contributes to the stabilization of the metallic state of LiOsO₃.

ACKNOWLEDGMENTS

We acknowledge financial support by the European Research Council under FP7/ERC Starting Independent Research Grant “SUPERBAD” (Grant Agreement No. 240524). Calculations have been performed at CINECA (HPC Project No. IsB06_SUPMOT).

[1] S. W. Cheong and M. Mostovoy, *Nat. Mater.* **6**, 13 (2007).

[2] D. Khomskii, *J. Magn. Magn. Mater.* **306**, 1 (2006).

[3] C. Ederer, T. Harris, and R. Kovacik, *Phys. Rev. B* **83**, 054110 (2011).

- [4] W. Luo, A. Franceschetti, M. Varela, J. Tao, S. J. Pennycook, and S. T. Pantelides, *Phys. Rev. Lett.* **99**, 036402 (2007).
- [5] P. W. Anderson and E. I. Blount, *Phys. Rev. Lett.* **14**, 217 (1965).
- [6] I. A. Sergienko, V. Keppens, M. McGuire, R. Jin, J. He, S. H. Curnoe, B. C. Sales, P. Blaha, D. J. Singh, K. Schwarz, and D. Mandrus, *Phys. Rev. Lett.* **92**, 065501 (2004).
- [7] M. Tachibana, N. Taira, H. Kawaji, and E. Takayama-Muromachi, *Phys. Rev. B* **82**, 054108 (2010).
- [8] T. Kolodiazny, M. Tachibana, H. Kawaji, J. Hwang, and E. Takayama-Muromachi, *Phys. Rev. Lett.* **104**, 147602 (2010).
- [9] I. K. Jeong, S. Lee, Se-Young Jeong, C. J. Won, N. Hur, and A. Llobet, *Phys. Rev. B* **84**, 064125 (2011).
- [10] Y. Shi, Y. Guo, X. Wang, A. J. Princep, D. Khalyavin, P. Manuel, Y. Michiue, A. Sato, K. Tsuda, S. Yu, M. Arai, Y. Shirako, M. Akaogi, N. Wang, K. Yamaura, and A. T. Boothroyd, *Nat. Mater.* **12**, 1024 (2013).
- [11] D. Puggioni and J. Rondinelli, *Nat. Commun.* **5**, 3432 (2014).
- [12] I. Inbar and R. E. Cohen, *Phys. Rev. B* **53**, 1193 (1996).
- [13] P. Hohenberg and W. Hohn, *Phys. Rev.* **136**, B864 (1964); W. Kohn and L. J. Sham, *ibid.* **140**, A1133 (1965).
- [14] G. Kresse and J. Furthmüller, *Phys. Rev. B* **54**, 11169 (1996); *Comput. Mater. Sci.* **6**, 15 (1996).
- [15] J. P. Perdew and A. Zunger, *Phys. Rev. B* **23**, 5048 (1981).
- [16] V. I. Anisimov, F. Aryasetiawan, and A. I. Lichtenstein, *J. Phys.: Condens. Matter* **9**, 767 (1997).
- [17] ISOTROPY Software Suite, <http://iso.byu.edu>.
- [18] Using the lattice vectors of the $R3c$ noncentrosymmetric experimental crystal structure the optimized Wyckoff positions are $z_{Li} = 0.88274$, $z_{Os} = 0.66651$ and $x_O = 0.29572$, $y_O = 0.33011$, $z_O = 0.25210$. The experimental Wyckoff positions are $z_{Li} = 0.88137$, $z_{Os} = 0.66667$ and $x_O = 0.29267$, $y_O = 0.32313$, $z_O = 0.25250$.
- [19] H. Sim and B. G. Kim, *Phys. Rev. B* **89**, 201107(R) (2014).
- [20] H. J. Xiang, *Phys. Rev. B* **90**, 094108 (2014).
- [21] The Wyckoff positions of the putative centrosymmetric structure are $z_{Li} = 0.91666$, $z_{Os} = 0.66666$ and $x_O = 0.29483$, $y_O = 0.33333$, $z_O = 0.25000$.
- [22] C. Capillas, E. S. Tasci, G. de la Flor, D. Orobengoa, J. M. Perez-Mato, and M. I. Aroyo, *Z. Krist.* **226**, 186 (2011).
- [23] R. E. Cohen and H. Krakauer, *Phys. Rev. B* **42**, 6416 (1990); R. Cohen, *Nature (London)* **358**, 136 (1992).
- [24] A. A. Mostofi, J. R. Yates, Y.-S. Lee, I. Souza, D. Vanderbilt, and N. Marzari, *Comput. Phys. Commun.* **178**, 685 (2008).
- [25] H. Shinaoka, T. Miyake, and S. Ishibashi, *Phys. Rev. Lett.* **108**, 247204 (2012).
- [26] R. Arita, J. Kunes, A. V. Kozhevnikov, A. G. Eguiluz, and M. Imada, *Phys. Rev. Lett.* **108**, 086403 (2012).
- [27] Y. Du, X. Wan, L. Sheng, J. Dong, and S. Y. Savrasov, *Phys. Rev. B* **85**, 174424 (2012).
- [28] Y. G. Shi, Y. F. Guo, S. Yu, M. Arai, A. A. Belik, A. Sato, K. Yamaura, E. Takayama-Muromachi, H. F. Tian, H. X. Yang, J. Q. Li, T. Varga, J. F. Mitchell, and S. Okamoto, *Phys. Rev. B* **80**, 161104(R) (2009).
- [29] B. J. Kim, Hosub Jin, S. J. Moon, J.-Y. Kim, B.-G. Park, C. S. Leem, Jaejun Yu, T. W. Noh, C. Kim, S.-J. Oh, J.-H. Park, V. Durairaj, G. Cao, and E. Rotenberg, *Phys. Rev. Lett.* **101**, 076402 (2008).